ACS OMEGA

http://pubs.acs.org/journal/acsodf

Article

CD44 Receptor-Targeted and Reactive Oxygen Species-Responsive H_2S Donor Micelles Based on Hyaluronic Acid for the Therapy of Renal Ischemia/Reperfusion Injury

Xiudi Zhou,[#] Qiang Chen,[#] Chunjing Guo, Yanguo Su, Huimin Guo, Min Cao, Zhongxin Liu, Dandan Zhang, Ningning Diao, Huaying Fan, and Daquan Chen*

Cite This: *ACS Omega* 2022, 7, 42339−42346

Read Online

ACCESS | Metrics & More | Article Recommendations

ABSTRACT: For the therapy attenuating renal ischemia−reperfusion (IR) injury, a novel drug delivery system was urgently needed, which could precisely deliver drugs to the pathological renal tissue. Here, we have prepared new nanomaterials with a reactive oxygen species (ROS)-responsive hydrogen sulfide (H_2S) donor and hyaluronic acid that targets CD44 receptor. The novel material was synthesized and characterized via related experiments. Then, rapamycin was loaded, which inhibited kidney damage. In the in vitro study, we found that the micelles had ROS-responsiveness, biocompatibility, and cell penetration. In addition, the experimental results showed that the intracellular H_2S concentration after administration was threefold higher than that of the control group. The western blot assay revealed that they have anti-inflammatory effects via H_2S donor blocking the NF-κB signaling pathway. Consequently, the rising CD44 receptor-targeting and ROS-sensitive H_2S donor micelles would provide a promising way for renal IR injury. This work provides a strategy for improving ischemia/reperfusion injury for pharmaceuticals.

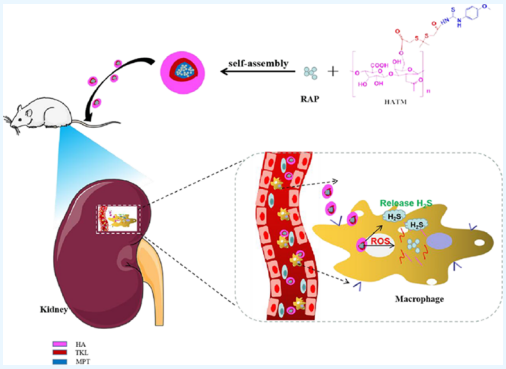

1. INTRODUCTION

Renal ischemia−reperfusion injury (IR), the major cause of acute kidney injury (AKI), is correlative with serious morbidity and mortality owing to reduced kidney function.[1] The AKI is strongly related to inflammatory cell recruitment, acidosis, or cell edema, which is caused by the decreasing adenosine triphosphate (ATP) and intensive reactive oxygen species (ROS).[2] The approaches in treating renal IR are to retard the progression of kidney disease, such as anti-inflammatory effects, blood pressure suppression, antianemia, antioxidation, antistress, and swelling inhibition approaches.[3] No effective pharmacological way has been reported to prevent or reverse the development of AKI. Studies have shown that macrophages, classified into M1 and M2, play a pivotal part in the initiation and development of kidney injury.[4,5] M1 cells as a proinflammatory phenotype produce abundant ROS, nitric oxide synthase, and other inflammation substances to mediate kidney tissue damage, while M2 cells are an anti-inflammatory phenotype, which repair the inflammation of tissue injury and fibrosis.[2] M2 cells mainly upregulate the expression of receptors on the cell membrane surface, such as CD44, CD206, CD163, and CD204.[6] Nevertheless, hyaluronic acid (HA) is a natural biopolysaccharide that specifically binds to the CD44 receptor and is involved in the adhesion and recruitment of macrophages.[5] In addition, HA, as a biodegradable and biocompatible material and skeleton structure of nanoparticles, has been accustomed to not only delivering the drug to the CD44 overexpression site but also improving its solubility, efficiency, and stability.[7]

Hydrogen sulfide (H_2S), an endogenous gasotransmitter, plays a major role in the regulation of tissue functions, such as the renal system, respiratory system, cardiovascular system, nervous system, and inflammatory system secondary to its anti-inflammatory, antiproliferative, antioxidative-stress, and antithrombotic effects.[8] The reasons for the amelioration of renal IR by H_2S may be ascribed to the following facts: (i) H_2S can steadily elevate the flow of renal blood and the rate of glomerular filtration with a mechanism likely inhibiting Na−K−2Cl and further excreting potassium and sodium;[9] (ii) H_2S reduces the concentration of ROS in endothelial cells owing to the lower nitric oxide xanthine level and superoxide;[10] (iii) H_2S strengthens the endogenous defense system by raising

Received: August 22, 2022
Accepted: October 31, 2022
Published: November 9, 2022

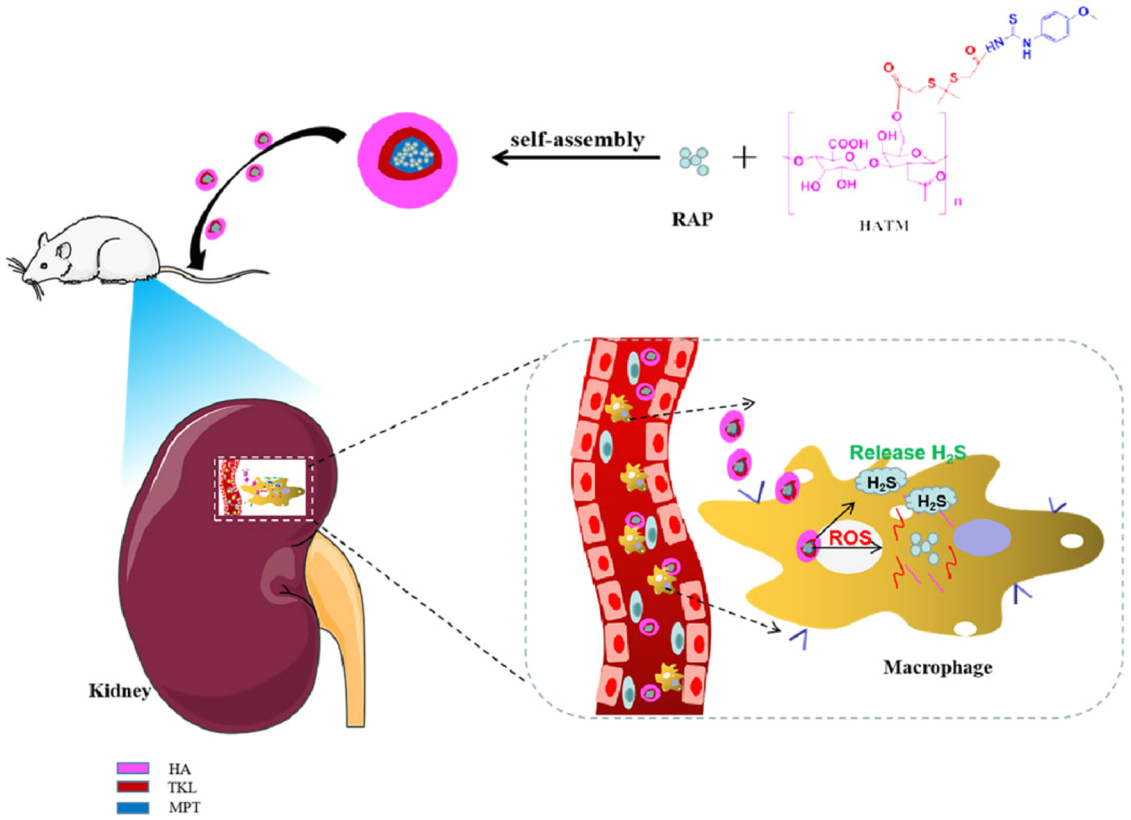

Figure 1. RAP release mechanism diagram of ROS-sensitive, H_2S-responsive, and CD44 receptor-targeting nanoparticles.

glutathione levels;[11] (iv) H_2S decreases the activation of nuclear factor kappa-light-chain-enhancer of activated B cells (NF-κB) and the expression of intracellular adhesion molecule 1 (ICAM-1);[12] and (v) H_2S blocks pyroptosis via inhibiting the NOD-, LRR-, and pyrin domain-containing protein 3 (NLRP3)/Caspase-1 axis.[13] 4-Methoxyphenyl thiourea (MPT) as a thiourea derivative can produce H_2S and may treat IR. ROS is a series of chemically reactive metabolites, including ClO^-, H_2O_2, O^{2-}, and so on. In ischemic injury, ROS generates oxidative stress and regulates certain signaling pathways, such as NF-κB, caspase-3, and p53.[14] The abundance of ROS damages human cells severely by disrupting organelles, cell membranes, and nuclear DNA if not eliminated by antioxidants.[15] Thioketal linkage (2′-[propane-2,2-diyllbls-(thio)]diacetic acl, TKL) is a hypersensitive ROS-responsive compound, which can be disrupted quickly at the inflammatory sites secondary to its high ROS concentration. In our previous research, we reported that TKL can be fractured in ROS conditions in atherosclerosis.[16] Rapamycin (RAP) is a hydrophobic drug with a weak oral bioavailability (about 14%), first observed as a macrolide antibacterial agent, which plays an important role in immunosuppression in organ transplantation, antifungal infection, antiproliferation, and antitumor functions.[17] RAP can prevent renal ischemia by its antiapoptotic effect and inhibition of tissue repair in renal IR.[14] Additionally, RAP can accelerate autophagy by the mTORC1/ATG13/ULK1 signaling pathway.[18] Thus, it has good potential in the therapy of renal IR.

At present, there are many ways for renal drug delivery. Cerium oxide nanoparticles,[19] nanopatricles,[14,20] gold particles,[21] SiO_2 nanospheres,[22] and lipid calcium phosphate gel[14] have been studied for improving hydrophobic drug solubility, raising accurate targeting, enhancing precision, declining adverse drug reactions, and multiple other uses. In this study, novel multifunctional nanoparticles were designed to treat IR injury, which had a critical treatment effect and superior potential. We prepared the multifunctional targeted NPs (HA−TKL-MPT HATM) by uniting CD44 receptors (HA) and ROS (TKL) with H_2S donor (MPT) and encapsulating RAP. Owing to the overexpression of CD44 at the site of kidney injury, HATM was anchored there. RAP was released apace secondary to high concentrations of ROS, while MPT released H_2S during systemic circulation (Figure 1). The characteristics of novel NP, cytotoxicity, cellular uptake, and therapeutic effect were investigated in vivo to measure the therapeutic potential of HATM@RAP NPs.

2. MATERIALS AND METHODS

2.1. Materials. HA was bought from Yuanye Biotechnology Co., Ltd. (China). RAP was purchased from Tokyo Pharmaron Industrial Co. (Japan). TKL was procured from Chuangyan Technology Co., Ltd. (China). MPT, 4-dimethylaminopyridine (DMAP), and dimethylformamide (DMF) were received from Shanghai Aladdin Biochemical Co., Ltd. (China). 1-Hydroxybenzotriazole hydrate (HOBT) was obtained from Shanghai Titan Co., Ltd. (China). Formamide was obtained from the OLBASE reagent net. All the reagents for the cell experiments were purchased from Solarbio (China).

2.2. Synthesis of HATM. TKL (67.2 mg) was added into 2 mL of formamide. Following this, EDC (114 mg) and DMAP (43.5 mg) were added and catalyzed at 35 °C for 2 h. HA (62.8 mg) was dissolved in 5 mL of formamide, added to the TKL solution in four drops (in 0.5 h-interval), and reacted at

https://doi.org/10.1021/acsomega.2c05407
ACS Omega 2022, 7, 42339−42346

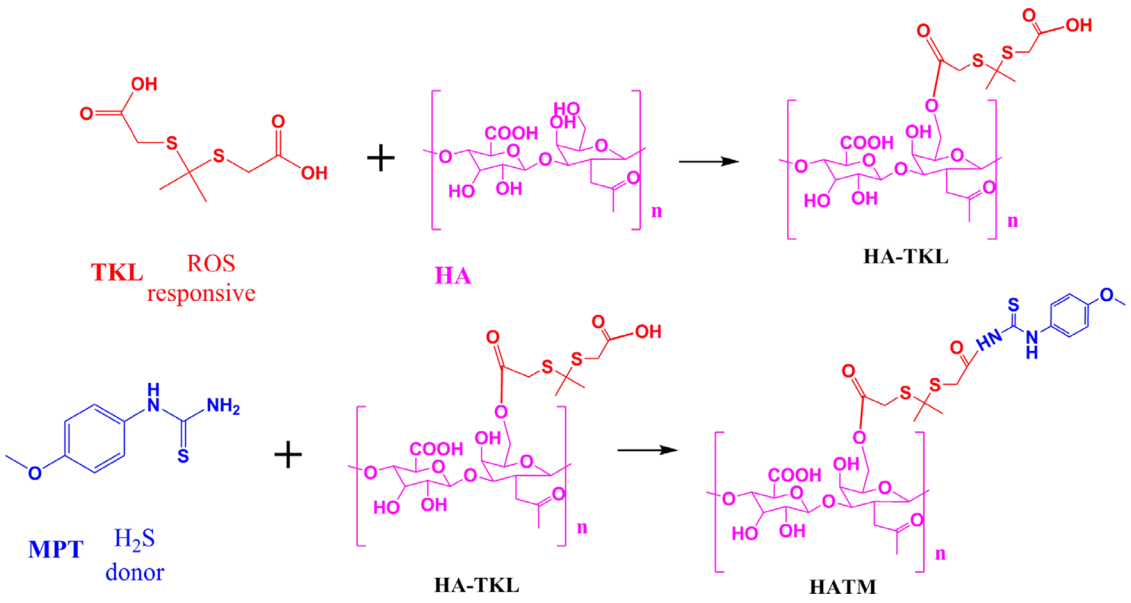

Figure 2. Chemical synthesis of HATM.

45 °C for 24 h. The mixture was dialyzed (MWCO = 3000 Da) for 48 h and freeze-dried to obtain HA−TKL.

MPT (54 mg), EDC (114 mg), and HOBT (81 mg) were mixed in 2 mL of DMF and catalyzed for 3 h at room temperature. One hundred milligrams of HA−TKL was dissolved in 3 mL of DMF and slowly dripped into MPT solution. Furthermore, the solution was reacted at homeothermy. Following 12 h, the solution was diluted (MWCO = 3000 Da) for 48 h and freeze-dried to obtain HATM (Figure 2).

2.3. Preparation of HATM@RAP Micelles. HATM (30 mg) and RAP (6 mg) were added to 3 mL of DMSO and stirred for 0.5 h to obtain a completely clear solution. Furthermore, the solution was dialyzed in the MWCO = 8000 Da dialysis bag and stirred for 48 h to obtain a micellar solution.

2.4. Characterization of HATM and HATM@RAP. Ten milligrams of HATM were dissolved in 0.6 mL of DMSO-D_6 and determined by proton nuclear magnetic resonance (^{1}H-NMR) spectra on a spectrometer (Bruker AV-500, Switzerland). Size, polymer dispersity index (PDI), and zeta potential were tested by DElsa Nano C (Beckman Colter, USA). A morphological investigation of HATM@RAP was done using a transmission electron microscope (TEM, H-600, Hitachi, Japan).

2.5. Determination of Encapsulation Rate (EE %) and Drug Load (DL %) of RAP in HATM@RAP. The consistency of RAP in micelles was evaluated by high-performance liquid chromatography at 277 nm with a UV detector. The mobile phase was acetonitrile:0.4% acetic acid solution (80:20), and the flow rate was 1 mL per minute at 35 °C.

$$\text{EE}\ (\%) = (\text{Weight of RAP in HATM@RAP})/(\text{Total RAP}) \times 100\%$$

$$\text{DL}\ (\%) = (\text{Weight of RAP in HATM@RAP})/(\text{Total HATM@RAP}) \times 100\%$$

2.6. In Vitro Determination of the ROS-Sensitive Property of HATM@RAP. In vitro release experiments were used to verify the ROS-sensitive properties of HATM@RAP by adding H_2O_2 at different concentrations. One milliliter HATM@RAP micellar solution containing 200 μg RAP was placed in dialysis bags with 20 mL of PBS solution (1% Tween 80, pH = 7.4) containing 0, 0.05, 0.5, or 5 mmol·L^{-1} H_2O_2, respectively. At this point, 100 μL of culture medium was removed, and an identical volume of fresh PBS solution was added. The concentration of RAP escaped from micelles was measured.

2.7. Cell Cultures. Renal mesangial cells or mouse macrophage RAW264.7 cells with extremely expressed CD44 receptors were grown in RPMI-1640 medium at 37 °C with 5% CO_2-saturated humidity.

2.8. Assays of Cytotoxicity of HATM. RAW 264.7 cells or renal mesangial cells were cultured in 96-well plates (5×10^4) for 12 h. Furthermore, various concentrations of HATM@RAP were added into wells and incubated for 12 or 24 h. Cell Counting Kit-8 (CCK-8) assay was adopted to measure cell viability.

2.9. Assays of Cell Internalization of HATM. RAW 264.7 cells or renal mesangial cells were cultured in 96-well plates (5×10^4) for 12 h. Cells were incubated for 12 h and then cultured with different concentrations of HATM@RAP for 0.5, 1, 2, and 4 h. Furthermore, cell uptake was observed using an inverted fluorescence microscope.

2.10. Determination of the Intracellular Concentration of H_2O_2. RAW 264.7 cells were incubated in six-well plates (1×10^6) for 12 h. Furthermore, the control group was disposed of with the latest medium, while other groups were stimulated with a fresh medium containing 100 ng/mL LPS for 2 h. Free RAP, HATM, and HATM@RAP were added separately and incubated. The intracellular concentration of H_2O_2 after 24 h was measured following the instructions provided by the Hydrogen Peroxide Assay Kit.

2.11. Determination of the Intracellular Generation of H_2S. RAW 264.7 cells were incubated in six-well plates (1×10^6) for 12 h. Furthermore, free RAP, HATM, and HATM@RAP were added separately and incubated for 24 h. The generating concentration of H_2S in cells was measured by a microsulfuretted hydrogen assay kit following its instructions.

https://doi.org/10.1021/acsomega.2c05407
ACS Omega 2022, 7, 42339−42346

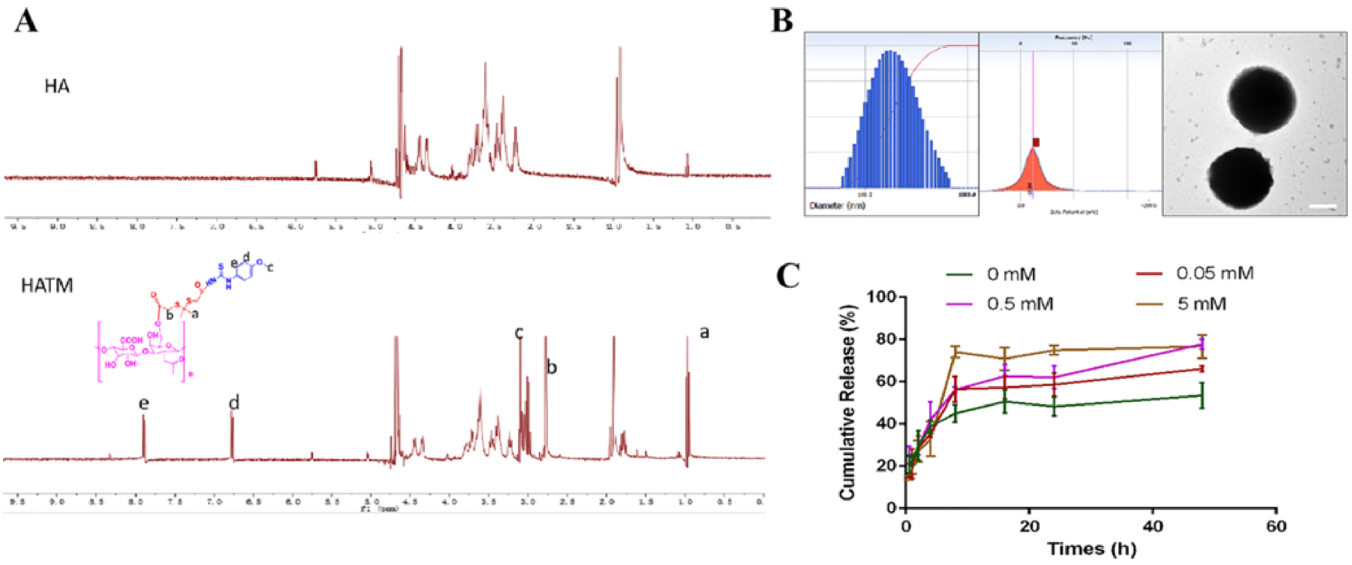

Figure 3. Characterization of HATM. (A) ^{1}H-NMR spectrum of HATM. (B) Particle size, zeta potential, and TEM picture of HATM. Scale bars, 100 nm. (C) ROS-sensitive drug releases of HATM in vitro.

2.12. Western Blot Assay. RAW264.7 cells were incubated in six-well plates (1×10^6) for 12 h. Furthermore, a control group was disposed of with the latest medium, while other groups were stimulated with a fresh medium containing 100 ng/mL LPS for 2 h. PBS, free RAP, HATM, and HATM@RAP were added separately and incubated. Following this, RAW264.7 cells were gathered and lysed in RIPA lysis buffer. Proteins were segregated in sodium dodecyl sulfate-polyacrylamide gel electrophoresis gel, delivered on a polyvinylidene fluoride membrane, incubated with primary antibodies of Bax and Bcl-2, and stored at 4 °C for 12 h. Furthermore, the membranes were hatched with the secondary antibodies at normal temperature for 2 h. Protein bands were visually advanced chemiluminescence substrates.

2.13. Treatment of IR Injury in Rats with HATM@RAP. Forty-two Sprague−Dawley rats were randomly assigned into six groups. Six groups (tribal groups) of animals underwent renal IR while the control group was without. In IR groups, the back was performed and clamps were used to occlude bilateral renal pedicle for 45 min. Furthermore, the renal pedicle was relaxed and rats were separately injected with normal saline, blank carrier (5 mg/kg), low-dose RAP (125 μg/kg), high-dose RAP (250 μg/kg), low-dose HATM@RAP (125 μg/kg), and high-dose HATM@RAP (250 μg/kg). Rats in each group were administered the corresponding substance once a day for 3 days after surgery. RAP was dissolved in a solution with 0.25% ethyl alcohol, 0.25% Tween 80, and 0.25% polyethylene glycol 400 in ultrapure water. They were euthanized 48 h following surgery.

2.14. Biochemical Analysis of Urinary Protein Levels. After euthanasia, urine was extracted by puncturing the bladder and stored at −20 °C instantly. Urinary protein, creatinine, and urea nitrogen (UN) levels were detected using homologous assay kits (Beyotime) according to the product manual.

2.15. Histological Analysis and Histopathological Examination. Major organs involving the liver, heart, lung, kidneys, and spleen were separated and stored at −20 °C. Furthermore, the five organs in each group were regularized with 4% paraformaldehyde, decorated in paraffin, and sectioned to a thickness of approximately 4 μg/mL. Hematoxylin−Eosin (H&E) staining was done on all five organ frozen sections while PAS staining was done only on the renal slice. The images were surveyed under a light microscope. Apoptosis of renal tubular epithelial cells was measured by TUNEL staining according to the explanatory memorandum. Renal slices were surveyed under a light microscope.

3. RESULTS AND DISCUSSION

3.1. Synthesis and Characterization of HATM. According to the above-mentioned method, a ROS-responsive H_2S donor nanomaterial (HATM) was successfully synthesized by NMR. The results presented in Figure 3A indicate principal peaks (in ppm) assigned to the MPT (δ 7.87, 3.10, and 6.76 ppm) and the TKL moiety (δ 0.94 and 2.57 ppm). The characteristic peaks of MPT and TKL were found in HATM. Thus, these results confirmed that HATM was triumphally synthesized.

3.2. Preparation and Characterization of HATM@RAP. As presented in Figure 3B, the average size of HATM@RAP was 169.21 ± 32.7 nm and the PDI was 0.233. The zeta potential of HATM was −18.84 ± 4.24 mV. TEM image revealed that particles were of spherical morphology without aggregation phenomenon. The EE % and DL % were 42.36 ± 7.68% and 7.06 ± 1.28%, respectively. These results demonstrated that the HATM@RAP was homogeneous and could be encapsulated appropriately. These results indicate the micelles were synthesized successfully.

To verify whether HATM had ROS-responsive characterization, drug release of RAP from HATM@RAP was evaluated in a solution with different H_2O_2 concentrations to simulate in vivo conditions (Figure 3). The release rate of RAP without H_2O_2 was 53.56 ± 5.94%, while those in the solutions with 0.05, 0.5, and 5 mM H_2O_2 concentrations were 66.17 ± 1.25, 77.86 ± 2.22, and 76.83 ± 5.50%. The results revealed that the release rate of RAP distinctly expedited in the presence of H_2O_2 and increased with the enhancement of H_2O_2 concentration. These results confirm that HATM has a good ROS-sensitive property. However, it was unsuitable for the in

https://doi.org/10.1021/acsomega.2c05407
ACS Omega 2022, 7, 42339−42346

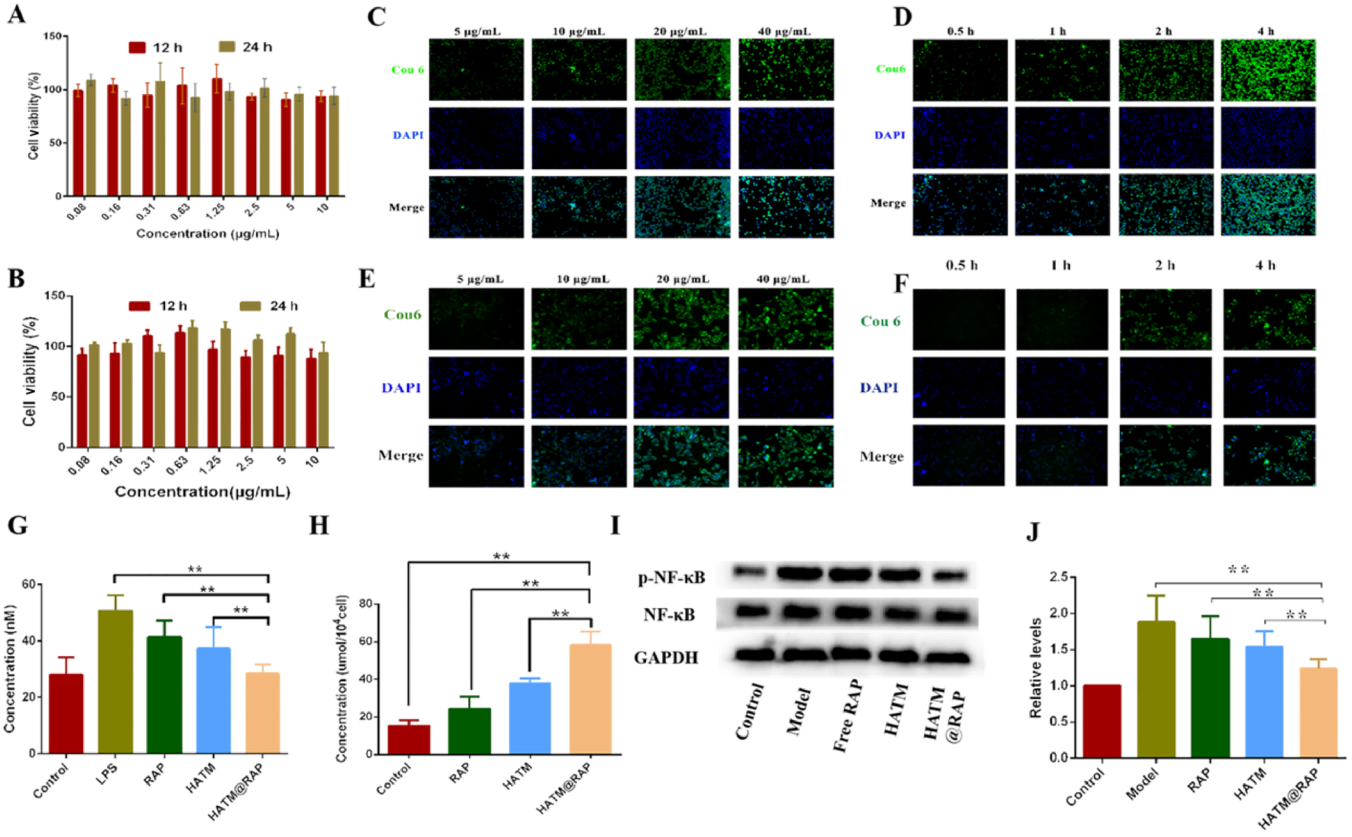

Figure 4. (A,B) Cytotoxicity of HATM@RAP for RAW264.7 cells and renal mesangial cells at 12 and 24 h. (C−F) Cell uptake of HATM@RAP for RAW264.7 cells and renal mesangial cells. (C) Concentration-dependent study of HATM in RAW264.7 cells. (D) Time-dependent study in RAW264.7 cells. (E) Result of the concentration-dependence study for renal mesangial cells. (F) Time-dependent study to renal mesangial cells. (G) Concentration of H_2O_2 in RAW264.7 cells after various groups (n = 3, mean ± SD). (H) Concentration of H_2S in RAW264.7 cells after various groups (n = 3, mean ± SD). (I) Representative Western blot bands of NF-κB and p-NF-κB after various groups. (J) Quantitative data of western blot of NF-κB and p-NF-κB (n = 3, mean ± SD). *P < 0.05, **P < 0.01.

vivo environment because human cells were liable to die when the concentration of ROS surpassed 1 mM.

3.3. In Vitro Cytotoxicity of HATM@RAP. In the development of originally targeted drug delivery systems, novel NPs must facilitate their clinical use by reducing the risk of harm.[23] To confirm the safety of RAP-loaded NPs, a CCK-8 assay was applied to examine the cytotoxicity of HATM@RAP at 12 or 24 h.[24] The cellular toxicity of novel NPs in different cells is related to the pathogenesis of macrophages and renal mesangial cells. As presented in Figure 4A,B, the cytotoxicity of HATM@RAP for 12 or 24 h with different RAP doses in macrophages and renal mesangial cells was higher than 90%. Additionally, there was no significant difference in cell toxicity between the dosing group and the control group (P > 0.05). The above results indicate that the micelles had no apparent toxicity on macrophages and renal mesangial cells.

3.4. In Vitro Cell Intracellular Delivery of HATM@RAP. Endocytosis of NPs is based on intracellular delivery of the loaded cargo molecules. Macrophages and renal mesangial cells have a significant effect on position-specific delivery of nanodrugs to renal IR. Therefore, cellular uptake behaviors in these two kinds of cells were investigated with a fluorescent inverted microscope. The results indicated that coumarin (Cou) labeled NPs were engulfed readily by two kinds of cells and spread out in the cytoplasm (Figure 4C−F). The uptake capacity of dosing at 40 μg/mL and hatch for 4 h was extremely higher than that in other groups. The results indicated that the novel NPs were an excellent drug carrier for transporting the drug into the two kinds of cells.

3.5. Determination of Intracellular H_2O_2 Concentration in RAW264.7 Cells. To verify the ROS-sensitive response of the novel NPs, H_2O_2 concentration in cells was determined by an H_2O_2 assay kit. The results revealed that H_2O_2 concentration in the LPS group was higher than that in other groups while the control group was rock-bottom (Figure 4G). H_2O_2 concentration in the HATM@RAP group was lower than that in the treatment groups albeit higher than that in the control group. These results revealed that the novel NPs had a remarkable ability to eliminate H_2O_2. The results showed that the HATM could reduce ROS compared with the LPS group. We think that it is due to the breakage of ROS-sensitive bonds scavenging a part of ROS, in addition to the possible H_2S production leading to the reduction of ROS.

3.6. Determination of Intracellular H_2S Concentration in RAW264.7 Cells. Determination of intracellular H_2S concentration was used to prove the function of H_2S generation from HATM@RAP. In comparison with the control group, RAP and HATM groups have further H_2S concentration (Figure 4H). Furthermore, the HATM@RAP group had the highest H_2S concentration. These results indicated that the novel NPs had a remarkable capacity to produce H_2S.

3.7. NF-κB Protein Expression in RAW264.7 Cells. RAP was efficient in IR through various mechanisms, such as NF-

https://doi.org/10.1021/acsomega.2c05407
ACS Omega 2022, 7, 42339−42346

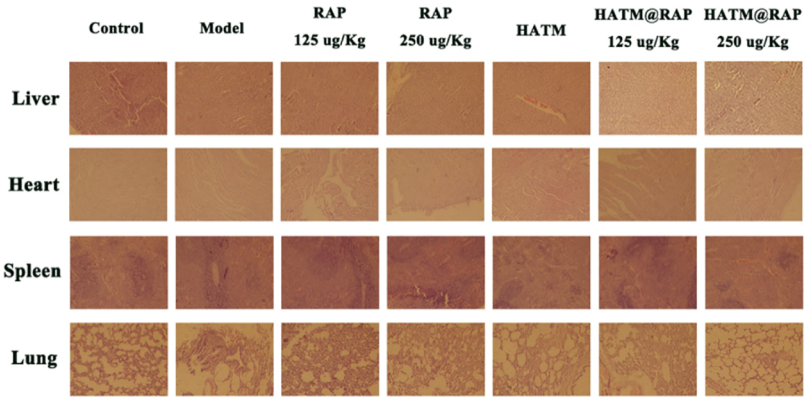

Figure 5. H&E stained sections of liver, heart, spleen, and lungs after various groups.

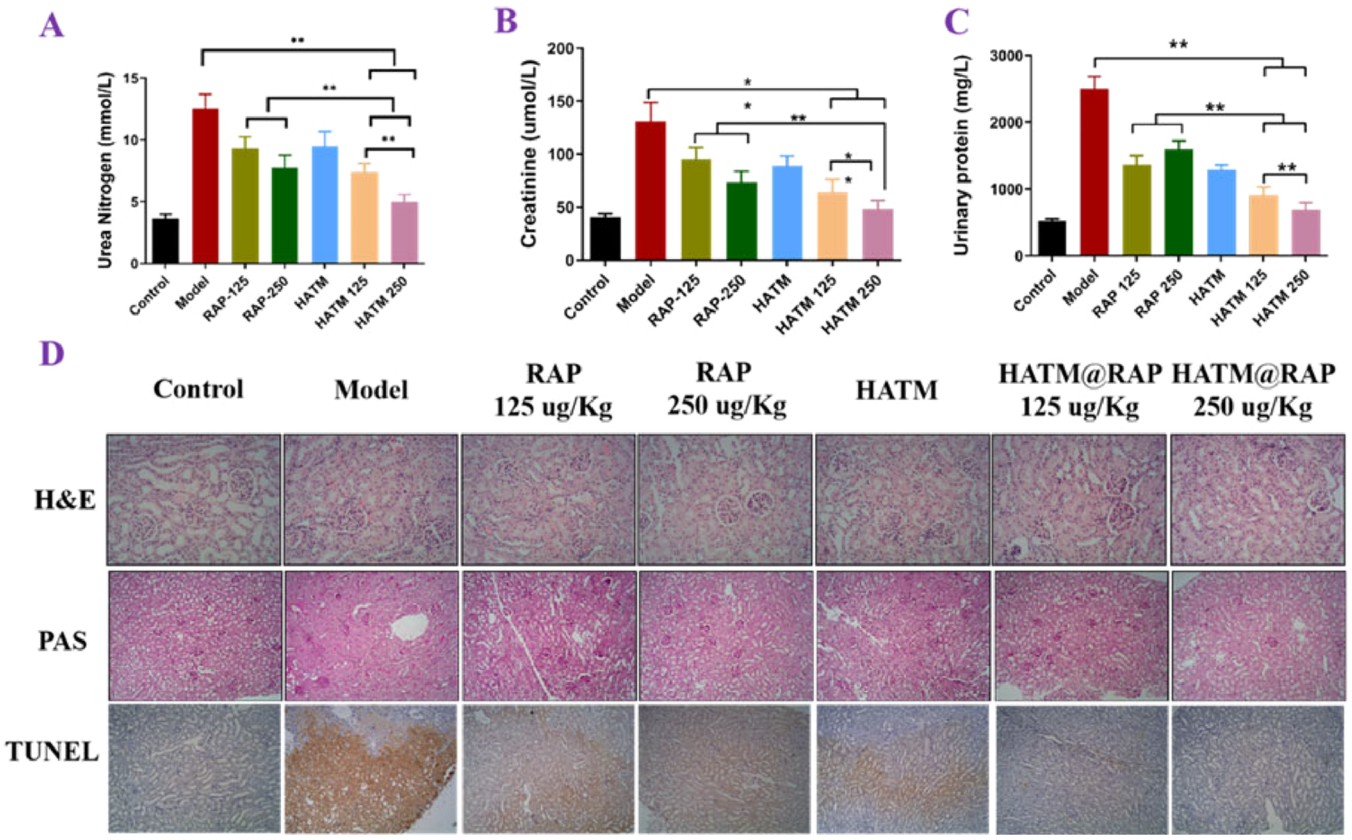

Figure 6. HATM@RAP could improve renal function in renal IRI rats. (A−C) Concentration of urea nitrogen (A), creatinine (B), and urinary protein (C) after various groups.*$P < 0.05$, **$P < 0.01$. (D) H&E, PAS, and TUNEL stains of each group in kidneys.

κB. To evaluate the inhibitory mechanism of HATM@RAP in inflammatory injury, we surveyed the NF-κB signaling pathway, which is probably related to the regulation of cytokine production. The results revealed that HATM@RAP lowered the level of p-NF-κB in RAW264.7 cells compared to the model, RAP, and HATM groups, which was higher than that in the control groups (Figure 4I,J). These results suggested that HATM@RAP reduced intracellular p-NF-κB concentration. The result reason could be that HATM inhibited the NF-κB signaling pathway via H_2S and ROS-responsive groups.

3.8. Biochemical Analysis. The poor solubility of RAP severely limited its application. However, RAP had numerous clinical effectiveness. Thus, various doses of RAP were used to verify the therapeutic effect. Creatinine, UN, and urinary protein were used to evaluate renal functions. As presented in Figure 6A−C, 3 days following administration, rats were euthanized and their bladder was punctured to extract urine samples, which were subsequently tested. The levels of creatinine, urea nitrogen, and urinary protein remarkably escalated in sham groups compared to those in the control group. Hence, it proved the success of the animal model experiment. Additionally, the high-dose HATM@RAP group revealed a significant effect by decreasing the three urine function levels compared to other groups. In addition, HE staining results of various organs showed that there was no obvious physiological toxicity (Figure 5).

3.9. Renal Histopathology. In recent years, HA-NPs were used as diagnostic or therapeutic agents for kidney inflammation. They accumulate at the site of inflammation

https://doi.org/10.1021/acsomega.2c05407
ACS Omega 2022, 7, 42339−42346

owing to their active targeting mechanism. In vivo, histopathology was used to test the therapeutic degree of the drug.

The normal cell structure of glomeruli and renal tubules was inspected through H&E and PAS stain (Figures 5 and 6D). Rat tissues in the control group revealed normal cell structures of glomeruli and renal proximal tubules and revealed protruding PAS-positive brush borders compared with those in the IR groups. The renal tissue of IR groups displayed that it underwent severe damage, such as edema, the disappearance of cell nuclear staining, luminal debris, cast formation, tubular necrosis, and inflammatory cell infiltration. The HATM@RAP group significantly ameliorated the symptoms of renal injury compared to other groups, indicating that the novel drug delivery system may be an excellent carrier for renal IR therapy.

4. CONCLUSIONS

Our study had four advantages. First, the novel NPs could target and accumulate to the CD44 receptor on the recruiting macrophages rapidly at the site of renal IR. Second, rapid drug release could be achieved because it could break down and release RAP with a high concentration of ROS. Third, it had the property of releasing H_2S slowly, owing to which a high concentration of H_2S could inhibit the progress of inflammation. Finally, it increased the solubility of RAP.

In summary, we developed a ROS-responsive H_2S donor nanocarrier with a CD44 receptor targeted to macrophages, which released RAP in a continuous manner triggered by H_2O_2. HATM@RAP entered macrophages and renal mesangial cells opportunely and smoothly reduced the intracellular H_2O_2 concentration, increased the intracellular H_2S concentration, and regulated the NF-κB signaling pathway. Therefore, it rectified the damage caused by renal inflammation. Our results suggest that HATM@RAP is a considerable drug delivery system with potential benefits for renal IR.

AUTHOR INFORMATION

Corresponding Author

Daquan Chen − *Collaborative Innovation Center of Advanced Drug Delivery System and Biotech Drugs, School of Pharmacy, Yantai University, Yantai 264005, P. R. China;* orcid.org/0000-0002-6796-0204; Email: cdq1981@1.26.com

Authors

Xiudi Zhou − *Collaborative Innovation Center of Advanced Drug Delivery System and Biotech Drugs, School of Pharmacy, Yantai University, Yantai 264005, P. R. China; Department of Pharmacy, Binzhou People's Hospital Affiliated to Shandong First Medical University, China, Binzhou 256600, P. R. China*

Qiang Chen − *Collaborative Innovation Center of Advanced Drug Delivery System and Biotech Drugs, School of Pharmacy, Yantai University, Yantai 264005, P. R. China;* orcid.org/0000-0002-7942-5292

Chunjing Guo − *College of Marine Life Science, Ocean University of China, Qingdao 266003, P. R. China*

Yanguo Su − *Collaborative Innovation Center of Advanced Drug Delivery System and Biotech Drugs, School of Pharmacy, Yantai University, Yantai 264005, P. R. China*

Huimin Guo − *Collaborative Innovation Center of Advanced Drug Delivery System and Biotech Drugs, School of Pharmacy, Yantai University, Yantai 264005, P. R. China*

Min Cao − *Collaborative Innovation Center of Advanced Drug Delivery System and Biotech Drugs, School of Pharmacy, Yantai University, Yantai 264005, P. R. China*

Zhongxin Liu − *Collaborative Innovation Center of Advanced Drug Delivery System and Biotech Drugs, School of Pharmacy, Yantai University, Yantai 264005, P. R. China*

Dandan Zhang − *Collaborative Innovation Center of Advanced Drug Delivery System and Biotech Drugs, School of Pharmacy, Yantai University, Yantai 264005, P. R. China*

Ningning Diao − *Collaborative Innovation Center of Advanced Drug Delivery System and Biotech Drugs, School of Pharmacy, Yantai University, Yantai 264005, P. R. China*

Huaying Fan − *Collaborative Innovation Center of Advanced Drug Delivery System and Biotech Drugs, School of Pharmacy, Yantai University, Yantai 264005, P. R. China*

Complete contact information is available at: https://pubs.acs.org/10.1021/acsomega.2c05407

Author Contributions

#Xiudi Zhou and Qiang Chen contributed equally to this study. Xiudi Zhou, Daquan Chen, and Huaying Fan designed the study, and Xiudi Zhou, Yanguo Su, and Huimin Guo carried out experiments; Xiudi Zhou, Qiang Chen, and Chunjing Guo analyzed the data; Xiudi Zhou made the figures, and Xiudi Zhou, Min Cao, Zhongxin Liu, Dandan Zhang, and Ningning Diao wrote the manuscript. All authors approved the final version of the manuscript.

Funding

This study was financially supported by Taishan Young Scholar Program (No. qnts20161035); Shandong Provincial Natural Science Foundation (No. ZR2019ZD24, ZR2019YQ30); Open fund project of the State Key Laboratory of Bio-Fibers and Eco-Textile (Qingdao University) (K2019-21); and Binzhou People's Hospital Affiliated to the first Medical University of Shandong (YBKTZR202119).

Notes

The authors declare no competing financial interest.

All procedures involving laboratory animals are performed by the ethics committee guidelines at Yantai University.

ACKNOWLEDGMENTS

The authors acknowledge the support of the Taishan Young Scholar Program, the Natural Science Foundation of Shandong Province, the Open fund project of the State Key Laboratory of Bio-Fibers and Eco-Textile (Qingdao University), and Binzhou people's Hospital Affiliated to the first Medical University of Shandong.

ABBREVIATIONS

IR, ischemia−reperfusion injury; H_2S, hydrogen sulfide; ROS, reactive oxygen species; HA, hyaluronic acid; RAP, rapamycin; TKL, 2′-[propane-2,2-diyllbls(thio)]diacetic acl; MPT, 4-methoxyphenyl thiourea; DMAP, 4-dimethylaminopyridine; HOBT, 1-hydroxybenzotriazole hydrate; ICAM-1, adhesion molecule 1

REFERENCES

(1) (a) Cao, H.; Cheng, Y.; Gao, H.; Zhuang, J.; Zhang, W.; Bian, Q.; Wang, F.; Du, Y.; Li, Z.; Kong, D.; et al. In Vivo Tracking of

https://doi.org/10.1021/acsomega.2c05407
ACS Omega 2022, 7, 42339−42346

Mesenchymal Stem Cell-Derived Extracellular Vesicles Improving Mitochondrial Function in Renal Ischemia-Reperfusion Injury. *ACS Nano* **2020**, *14*, 4014−4026. (b) Dwyer, K. M.; Kishore, B. K.; Robson, S. C. Conversion of extracellular ATP into adenosine: a master switch in renal health and disease. *Nat. Rev. Nephrol.* **2020**, *16*, 509−524. (c) Huang, C. L.; Zeng, T.; Li, J. W.; Tan, L. S.; Deng, X. L.; Pan, Y. C.; Chen, Q.; Li, A. Q.; Hu, J. Q. Folate Receptor-Mediated Renal-Targeting Nanoplatform for the Specific Delivery of Triptolide to Treat Renal Ischemia/Reperfusion Injury. *ACS Biomater. Sci. Eng.* **2019**, *5*, 2877−2886. (d) Wang, S.; Liu, A.; Wu, G.; Ding, H. F.; Huang, S.; Nahman, S.; Dong, Z. The CPLANE protein Intu protects kidneys from ischemia-reperfusion injury by targeting STAT1 for degradation. *Nat. Commun.* **2018**, *9*, 1234.

(2) Wang, Y.; Cui, J.; Liu, M.; Shao, Y.; Dong, X. Schisandrin C attenuates renal damage in diabetic nephropathy by regulating macrophage polarization. *Am. J. Transl. Res.* **2021**, *13*, 210−222.

(3) Zhang, T.; Guo, J. R.; Gu, J.; Chen, K.; Li, H. L.; Wang, J. L. Protective Role of mTOR in Liver Ischemia/Reperfusion Injury: Involvement of Inflammation and Autophagy. *Oxid. Med. Cell. Longevity* **2019**, *2019*, No. 7861290.

(4) (a) Carcy, R.; Cougnon, M.; Poet, M.; Durandy, M.; Sicard, A.; Counillon, L.; Blondeau, N.; Hauet, T.; Tauc, M. Targeting oxidative stress, a crucial challenge in renal transplantation outcome. *Free Radical Biol. Med.* **2021**, *169*, 258−270. (b) Roorda, M.; Miljkovic, J. L.; van Goor, H.; Henning, R. H.; Bouma, H. R. Spatiotemporal regulation of hydrogen sulfide signaling in the kidney. *Redox Biol.* **2021**, *43*, No. 101961.

(5) (a) T, P. M. K.; Nikolic-Paterson, D. J.; Lan, H. Y. Macrophages: versatile players in renal inflammation and fibrosis. *Nat. Rev. Nephrol.* **2019**, *15*, 144−158. (b) Vegting, Y.; Vogt, L.; Anders, H. J.; De Winther, M. P. J.; Bemelman, F. J.; Hilhorst, M. L. Monocytes and macrophages in ANCA-associated vasculitis. *Autoimmun. Rev.* **2021**, *20*, No. 102911.

(6) Chen, D.; Lian, S.; Sun, J.; Liu, Z.; Zhao, F.; Jiang, Y.; Gao, M.; Sun, K.; Liu, W.; Fu, F. Design of novel multifunctional targeting nano-carrier drug delivery system based on CD44 receptor and tumor microenvironment pH condition. *Drug Delivery* **2016**, *23*, 808−803.

(7) Wang, B. J.; Zhang, W.; Zhou, X. D.; Liu, M. N.; Hou, X. Y.; Cheng, Z. T.; Chen, D. Q. Development of dual-targeted nano-dandelion based on an oligomeric hyaluronic acid polymer targeting tumor-associated macrophages for combination therapy of non-small cell lung cancer. *Drug Delivery* **2019**, *26*, 1265−1279.

(8) Wang, K.; Guo, C.; Dong, X.; Yu, Y.; Wang, B.; Liu, W.; Chen, D. In Vivo Evaluation of Reduction-Responsive Alendronate-Hyaluronan-Curcumin Polymer-Drug Conjugates for Targeted Therapy of Bone Metastatic Breast Cancer. *Mol. Pharmaceutics* **2018**, *15*, 2764−2769.

(9) (a) Hashmp, S. F.; Sattar, M. Z. A.; Rathore, H. A.; Ahmadi, A.; Johns, E. J. A critical review on pharmacological significance of hydrogen sulfide (H(2)S) ON NF-kappaB concentration and ICAM-1 expression in renal ischemia reperfusion injury. *Acta Pol. Pharm.* **2017**, *74*, 747−752. (b) Chen, Q.; Guo, C.; Zhou, X.; Su, Y.; Guo, H.; Cao, M.; Li, J.; Zhang, Y.; Zhao, W.; Gao, X.; et al. N-acetylneuraminic acid and chondroitin sulfate modified nanomicelles with ROS-sensitive H(2)S donor via targeting E-selectin receptor and CD44 receptor for the efficient therapy of atherosclerosis. *Int. J. Biol. Macromol.* **2022**, *211*, 259−270.

(10) Smagliy, L. V.; Gusakova, S. V.; Birulina, Y. G.; Kovalev, I. V.; Orlov, S. N. The Role of Hydrogen Sulfide in Volume-Dependent Mechanisms of Regulation of Vascular Smooth Muscle Cells Contractile Activity. *Ross. Fiziol. Zh. im. I. M. Sechenova* **2015**, *101*, 441−450.

(11) Modis, K.; Coletta, C.; Erdelyi, K.; Papapetropoulos, A.; Szabo, C. Intramitochondrial hydrogen sulfide production by 3-mercaptopyruvate sulfurtransferase maintains mitochondrial electron flow and supports cellular bioenergetics. *FASEB J.* **2013**, *27*, 601−611.

(12) Kimura, Y.; Goto, Y.; Kimura, H. Hydrogen sulfide increases glutathione production and suppresses oxidative stress in mitochondria. *Antioxid. Redox Signaling* **2010**, *12*, 1−13.

(13) Sun, H. J.; Leng, B.; Wu, Z. Y.; Bian, J. S. Polysulfide and Hydrogen Sulfide Ameliorate Cisplatin-Induced Nephrotoxicity and Renal Inflammation through Persulfidating STAT3 and IKK beta. *Int. J. Mol. Sci.* **2020**, *21*, 7805.

(14) (a) Ke, J.; Cai, G. Effect of IL-33 on pyroptosis of macrophages in mice with sepsis via NF-kappaB/p38 MAPK signaling pathway. *Acta Cir. Bras.* **2021**, *36*, No. e360501. (b) Zhao, H. H.; Han, Q. X.; Ding, X. N.; Yan, J. Y.; Li, Q.; Zhang, D.; Zhu, H. Y. Critical hubs of renal ischemia-reperfusion injury: endoplasmic reticulum-mitochondria tethering complexes. *Chin. Med. J.* **2020**, *133*, 2599−2609.

(15) Liu, Z.; Liu, X.; Yang, Q.; Yu, L.; Chang, Y.; Qu, M. Neutrophil membrane-enveloped nanoparticles for the amelioration of renal ischemia-reperfusion injury in mice. *Acta Biomater.* **2020**, *104*, 158−166.

(16) Chen, W.; Li, D. Reactive Oxygen Species (ROS)-Responsive Nanomedicine for Solving Ischemia-Reperfusion Injury. *Front. Chem.* **2020**, *8*, 732.

(17) Hou, X.; Lin, H.; Zhou, X.; Cheng, Z.; Li, Y.; Liu, X.; Zhao, F.; Zhu, Y.; Zhang, P.; Chen, D. Novel dual ROS-sensitive and CD44 receptor targeting nanomicelles based on oligomeric hyaluronic acid for the efficient therapy of atherosclerosis. *Carbohydr. Polym.* **2020**, *232*, No. 115787.

(18) Mugume, Y.; Kazibwe, Z.; Bassham, D. C. Target of Rapamycin in Control of Autophagy: Puppet Master and Signal Integrator. *Int. J. Mol. Sci.* **2020**, *21*, 8259.

(19) Miricescu, D.; Balan, D. G.; Tulin, A.; Stiru, O.; Vacaroiu, I. A.; Mihai, D. A.; Popa, C. C.; Papacocea, R. I.; Enyedi, M.; Sorin, N. A.; et al. PI3K/AKT/mTOR signalling pathway involvement in renal cell carcinoma pathogenesis (Review). *Exp. Ther. Med.* **2021**, *21*, 540.

(20) Stephen Inbaraj, B.; Chen, B. H. An overview on recent in vivo biological application of cerium oxide nanoparticles. *Asian J. Pharm. Sci.* **2020**, *15*, 558−575.

(21) Deng, X.; Zeng, T.; Li, J.; Huang, C.; Yu, M.; Wang, X.; Tan, L.; Zhang, M.; Li, A.; Hu, J. Kidney-targeted triptolide-encapsulated mesoscale nanoparticles for high-efficiency treatment of kidney injury. *Biomater. Sci.* **2019**, *7*, 5312−5323.

(22) Tartuce, L. P.; Brandt, F. P.; Pedroso, G. D.; Farias, H. R.; Fernandes, B. B.; Pereira, B. D.; Machado, A. G.; Feuser, P. E.; Silveira, P. C. L.; Nesi, R. T.; et al. 2-methoxy-isobutyl-isonitrile-conjugated gold nanoparticles improves redox and inflammatory profile in infarcted rats. *Colloids Surf., B* **2020**, *192*, No. 111012.

(23) Zheng, Z.; Deng, G.; Qi, C.; Xu, Y.; Liu, X.; Zhao, Z.; Zhang, Z.; Chu, Y.; Wu, H.; Liu, J. Porous Se@SiO2 nanospheres attenuate ischemia/reperfusion (I/R)-induced acute kidney injury (AKI) and inflammation by antioxidative stress. *Int. J. Nanomed.* **2019**, *14*, 215−229.

(24) Li, H.; Teng, Y.; Xu, X.; Liu, J. Enhanced rapamycin delivery to hemangiomas by lipid polymer nanoparticles coupled with anti-VEGFR antibody. *Int. J. Mol. Med.* **2018**, *41*, 3586−3596.

https://doi.org/10.1021/acsomega.2c05407
ACS Omega 2022, 7, 42339−42346